Colloid Polym Sci (2008) 286:873–879
DOI 10.1007/s00396-007-1829-z

ORIGINAL CONTRIBUTION

Synthesis and characterization of side-chain liquid-crystalline polysiloxanes containing fluorinated units

Fan-Bao Meng · Yong-Mei Gao · Jiao Lian · Bao-Yan Zhang · Feng-Zhen Zhang

Received: 15 October 2007 / Accepted: 10 December 2007 / Published online: 11 March 2008

Abstract Several new chiral side-chain LC polysiloxanes (**IP–VIIP**) bearing fluorinated methyl groups were synthesized with a cholesteric LC monomer and a non-LC monomer containing fluorinated units. The chemical structures and LC properties of the monomers and polymers were characterized by use of various experimental techniques. The effect of copolymer composition on mesomorphic properties of the fluorine-containing polymers was studied as well. The obtained polymers were soluble in many solvents and the specific rotations showed negative values. The temperatures at which 5% weight loss occurred (T_d) were greater than 300 °C for all the polymers and the residue weight on heating to 600 °C increased slightly with increase of the monomer containing fluorinated units in the polymer systems. All the polymers displayed two-phase transitions when they were heated and cooled. The **IP**, **IIP**, and **IIIP** exhibited cholesteric textures when they were heated and cooled, while **IVP**, **VP**, **VIP**, and **VIIP** showed smectic fan-shaped textures. XRD curves of samples of **IVP**, **VP**, **VIP**, and **VIIP** displayed sharp and strong peaks at low angle, but no sharp peaks were shown at low angle for the samples **IP**, **IIP**, and **IIIP**.

Keywords Liquid-crystalline polymers · Fluorinated polymers · Mesophase · Chiral

Introduction

Fluorinated polymers show lots of outstanding properties such as low dielectric constant, low refractive index and high optical transparency, as well as chemical and thermal resistance. They represent a class of very interesting and versatile polymeric materials that may find application in many different fields ranging from electronics and optics to coatings. The incorporation of fluorine in a polymer causes the polymer to have a low surface energy potentially leading to low wettability, low friction coefficient and low adhesion. Fluorinated liquid-crystalline polymers (FLCPs) are a relatively new class of fluoropolymers [1–7]. Fluorine's small size, large electronegativity, low polarizability, and large fluorine–fluorine repulsion lead to many interesting properties of FLCPs. The introduction and the choice of the fluorine atom position within liquid crystal systems allow formation of materials that present a considerable technological interest for display or non-display applications [8].

Initial studies on fluorinated liquid crystals focused on partly fluorinated alkanes such as diblock hydrocarbon–fluorocarbon molecules. Appropriately fluorinated molecules may be conceived as unconventional mesogens in that they do not possess the usual molecular features of more traditional liquid crystals. These compounds showed liquid-crystalline mesophases presumably due to the strong phase separation of fluorocarbon from hydrocarbon chain segments and also to the rigid rod-like nature of the fluorocarbon chains that tend to adopt a helical conformation in the mesophase state [9–13]. Later synthetic efforts resulted in the development of liquid-crystalline polymers in which the length of the fluorinated tail was varied [14–16]. More conventional mesogenic units have also been used in combination with partly fluorinated tails in polymeric liquid crystals [17–19]. The involvement is generally obtained from the introduction of fluorine onto the rigid core, so-called fluoro-substituents [20]. In fact, the properties required are those for materials used in the electronic industry: optical and chemical stability, wide

F.-B. Meng · Y.-M. Gao · J. Lian · B.-Y. Zhang (✉) · F.-Z. Zhang
The Research Centre for Molecular Science and Engineering,
Northeastern University,
Shenyang 110004, People's Republic of China
e-mail: byzcong@163.com

mesomorphic temperature range, low melting point, low viscosity, and low conductivity.

On the other hand, chiral materials have been an extensively studied area because of their unique properties, which are directly related to the atomic chiral centers and helical conformations. When molecular chirality is introduced into LCPs, chiral LC phases having helical morphology are induced, resulting in a series of potential applications in optics and electro-optics [21–23]. Chiral LCPs may exhibit a marvelous variety of liquid-crystalline phases, including the chiral smectic C^* phase, the cholesteric phase, and the blue phases [24–26]. Recently, chiral side-chain LCPs composed of chiral mesogens have attracted both industrial and scientific interests, because their additional properties such as piezoelectricity, ferroelectricity, and pyroelectricity result from the symmetry breaking brought by molecular chirality [27].

To achieve a better understanding of liquid crystal phase behavior of chiral LCPs containing fluorinated groups, we are interested in side-chain LCPs containing both chiral and fluorinated methyl groups. In the present study, we synthesize a series of polysiloxane-based chiral side-chain FLCPs using cholesteryl and fluorinated monomers (Fig. 1).

Experimental

Materials

4-Hydroxybenzoic acid, cholesterol, bromopropene, 3-trifluoromethyl-phenol, undec-10-enoic acid, poly(methylhydrogeno)siloxane (PMHS) (Mn ≈ 600) and hexachloroplatinic acid hydrate were obtained from Jilin Chemical Industry Company and used without any further purification. Pyridine, thionyl chloride, toluene, ethanol, chloroform, tetrahydrofuran (THF) and methanol were purchased from Shenyang Chemical Co. Pyridine was purified by distillation over KOH and NaH before using.

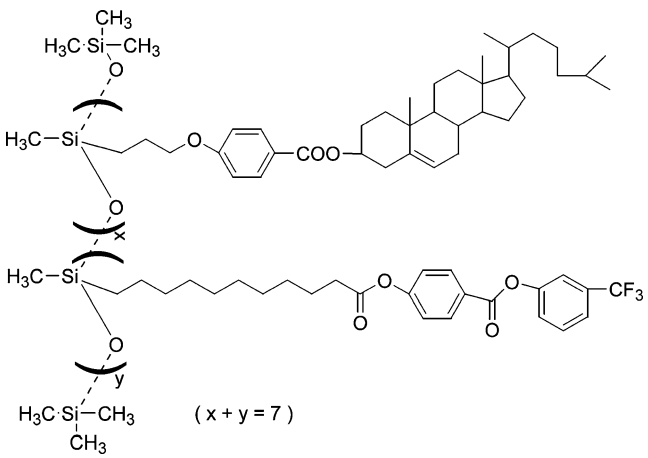

Fig. 1 The general structures of the liquid-crystalline polymers

Characterization

FTIR spectra of the synthesized polymers and monomers were obtained by the KBr method performed on PerkinElmer instruments Spectrum One Spectrometer (PerkinElmer, Foster City, CA). ^{1}H NMR (300 MHz) spectrum was obtained with a Varian Gemini 300 NMR Spectrometer (Varian Associates, Palo Alto, CA) with tetramethylsilane (TMS) as an internal standard. The element analysis (EA) of monomers and polymers was carried out by use of an Elementar Vario EL III (Elementar, Germany). Thermal transition properties were characterized by a NETZSCH instrument DSC 204 (Netzsch, Wittelsbacherstr, Germany) at a heating rate of 10 °C min^{-1} under nitrogen atmosphere. The thermal stability of the polymers under atmosphere was measured with a NETZSCH TGA 209C thermogravimetric analyzer. Visual observation of liquid-crystalline transitions and optical textures under cross-polarized light was made using a Leica DMRX (Leica, Wetzlar, Germany) POM equipped with a Linkam THMSE-600 (Linkam, Surrey, England) hot stage. X-ray measurements of the samples were performed using Cu Kα(λ=1.542 Å) radiation monochromatized with a Rigaku DMAX-3A X-ray diffractometer (Rigaku, Japan). The samples were placed on a substrate glass and heated to their mesophase temperatures, then quenched with cold water to obtain films of corresponding samples. The sample is then heated at 10 °C min^{-1} at the desired experimental temperature and left to equilibrate for 10 min at this temperature before starting the experiment. Gel permeation chromatography (GPC) measurements were carried out in THF on a Waters 2410 instrument equipped with three Waters μ-Styragel columns (10^3, 10^4, and 10^5 Å) at 35 °C, with a Waters 2410 RI detector. Calibration was made with standard polystyrene. The number-averaged molecular weight (M_n) of the polymers was calibrated by reference to a universal calibration curve and polystyrene standards in THF at 35 °C. Measurement of optical rotation (α) was carried out with a PerkinElmer instrument Model 341 Polarimeter using the D line of a sodium vapour lamp.

Synthesis

The intermediate product 4-undec-10-enoyloxy-benzoyl chloride and the chiral LC monomer cholest-5-en-3-ol (3β)-4-(2-propenyloxy)benzoate (**M1**) were synthesized according to our previous reports [28, 29].

3-Trifluoromethyl-phenol (16.2 g, 0.10 mol) and 18 ml pyridine were dissolved in 250 ml dry THF to which the 4-undec-10-enoyloxy-benzoyl chloride (32.2 g, 0.10 mol)

was added dropwise at 25 °C. The reaction mixture was stirred at room temperature for 2 h, then heated to 60 °C and kept for 18 h in a water bath to ensure that the reaction finished. Then 200 ml of THF was distilled out. After cooling to room temperature, the residue was poured into 500 ml cold water. The precipitates were isolated by filtration and dried in a vacuum oven. Recrystallization in alcohol results in a brown wax of 3-trifluoromethyl-phenyl 4-undec-10-enoyloxy-benzoate (**M2**, yield: 90%); mp 21–22 °C.

^{1}H NMR ($CDCl_3$): δ (ppm)=0.96–2.28 (16 H, m, alkane-*H*); 4.87 (2H, d, *J*=3.6 Hz, C*H*$_2$=6;CH–); 6.02–6.12 (1 H, m, CH$_2$=6;C*H*–); 7.11 (3H, d, *J*=9.3 Hz, Ar-*H*); 7.2–7.31 (3H, m, Ar-*H*); 8.13 (2H, d, *J*=20.4 Hz, Ar-*H*).

FTIR (KBr,): ν (cm^{-1})=3077, 2929, 2856 (C–H aliphatic), 1761–1710 (C=6;O in different ester linkages), 1605, 1505 (Ar), 1257 (C–F).

Elem. Anal. Calcd. for $C_{25}H_{27}F_3O_4$: C, 66.95%; H, 6.07%; F, 12.71. Found: C, 67.03; H, 6.09; F, 12.81.

For synthesis of polymers **IP**–**VIIP**, the same method was adopted. The polymerization experiments were summarized in Table 1. The synthesis of polymer **VIP** was given as an example. Chiral liquid-crystalline monomer **M1** (2.95 g, 5.4 mmol) was dissolved in 150 ml of dry, fresh distilled toluene. To the stirred solution, fluorinated LC monomer **M2** (0.72 g, 1.6 mmol), PMHS (0.59 g, 1.0 mmol) and 2 ml of H_2PtCl_6/THF (0.50 g hexachloroplatinic acid hydrate dissolved in 100 ml THF) were added and heated under nitrogen and anhydrous conditions at 65–68 °C for 30 h. Then the mixture was cooled and poured into methanol. After filtration, the product was dried at 80 °C for 4 h under vacuum to obtain polymer in the yield of 80%.

FTIR (KBr): ν (cm^{-1})=2933, 2868 (C–H aliphatic), 1706 (C=6;O), 1608, 1511 (Ar), 1259 (C–F), 1011–1105 (Si–O).

Elem. Anal. Found: C, 70.48; H, 9.28; F, 2.14.

Results and discussion

Synthesis

The chemical structures of **M1** and **M2** were characterized with IR and ^{1}H NMR spectra, which was in good agreement with the prediction. The spectra of **M1** and **M2** suggest that the purity is high and this was confirmed by EA.

Polymers **IP**–**VIIP** were prepared by a one-step hydrosilylation reaction between Si–H groups of PMHS and olefinic C=6;C of **M1** and **M2** in toluene, with hexachloroplatinate as a catalyst. The obtained polymers were soluble in toluene, xylene, THF, chloroform, and so forth. But their solubility varied with different solvents such as toluene and THF (Table 1). This result means that the polarity of the polymers varied with increasing of fluorinated units in the polymer systems. The M_n of the synthesized polymers was measured on a GPC instrument. GPC curves of the polymers were symmetrically single modal, and the data were listed in Table 1, indicating that the M_n decreased slightly with increase of **M2** feed in polymerization. All the polymers were characterized by IR spectra and elementary analysis. Polymer **VIP** contains the representative features for all of the polymers. The characteristic absorption bands are as follows: 2933–2868 cm^{-1} (C–H stretching), 1730–1706 cm^{-1} (C=6;O stretching), 1608 and 1511 cm^{-1} (C=6;C stretching of aromatic nucleus), 1259 cm^{-1} (C–F stretching), and 1011–1105 (Si–O stretching). For the polysiloxanes, the disappearance of the PMHS Si–H stretching at 2160 cm^{-1} and the appearance of characteristic absorption bands of monomers indicate successful incorporation of monomers into the polysiloxane chains. Mass percentage of the fluorine atom in the polymer systems was characterized with EA measurements and the data were listed in Table 1. It showed that the mass percentage of fluorine atom increased with increase of monomer **M2** in

Table 1 Polymerization and some properties of the polymers

Sample	Feed			M_n[a] (×10^{-3})	% F[b]	Solubility[c]		Specific rotation[d]
	PMHS (mmol)	M1 (mmol)	M2 (mmol)			Toluene	THF	
IP	1.0	6.95	0.05	4.46	0.06	+++++	+++++	−12.30
IIP	1.0	6.9	0.1	4.45	0.13	+++++	+++++	−12.28
IIIP	1.0	6.8	0.2	4.39	0.26	++++	+++++	−11.56
IVP	1.0	6.6	0.4	4.36	0.52	+++	+++++	−11.13
VP	1.0	6.2	0.8	4.32	1.05	+++	+++++	−10.47
VIP	1.0	5.4	1.6	4.24	2.14	++	+++++	−9.43
VIIP	1.0	3.8	3.2	4.09	4.45	+	+++++	−8.11

[a] Measured on water-2410 GPC instrument.
[b] Mass percentage of fluorine atom in the polymer systems, obtained from element analysis (EA) of the polymers.
[c] The more +, the better solubility in solvent.
[d] Specific rotation of polymers $\left([\alpha]_D^{20}\right)$, 0.1 g in 50 mL THF.

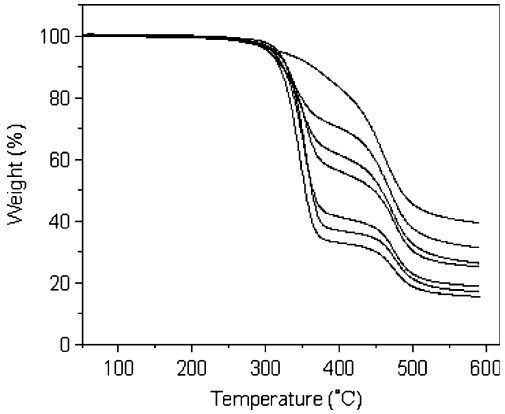

Fig. 2 TGA thermograms of **VIIP–IP** (*from the top down*)

the polymers corresponding with the feed. The specific rotations of the chiral liquid-crystalline polymers were also listed in Table 1. As compared with monomers **M1** ([α]= −30.1°), the polymers showed lower specific rotation absolute values. It indicated that cleavage of the double bond and the binding of monomers to the polysiloxane main chains affect the chirality of the polymers. Furthermore, the specific rotation of polymers from **IP** to **VIIP** revealed a similar tendency, i.e., the specific rotation absolute values decreasing with increase of **M2** component in the polymer systems, suggesting the decrease of chiral components.

Thermal analysis

TGA thermograms of the representative polymers (Fig. 2) and TGA values (Table 2) showed that the temperatures at which 5% weight loss occurred (T_d) were greater than 300 °C for all the polymers, suggesting high thermal stability. The T_d and the residue weight of the samples on heating to 600 °C increased slightly from **IP** to **VIIP**, indicating increased thermal stability with increase of fluorinated units in the polymer systems.

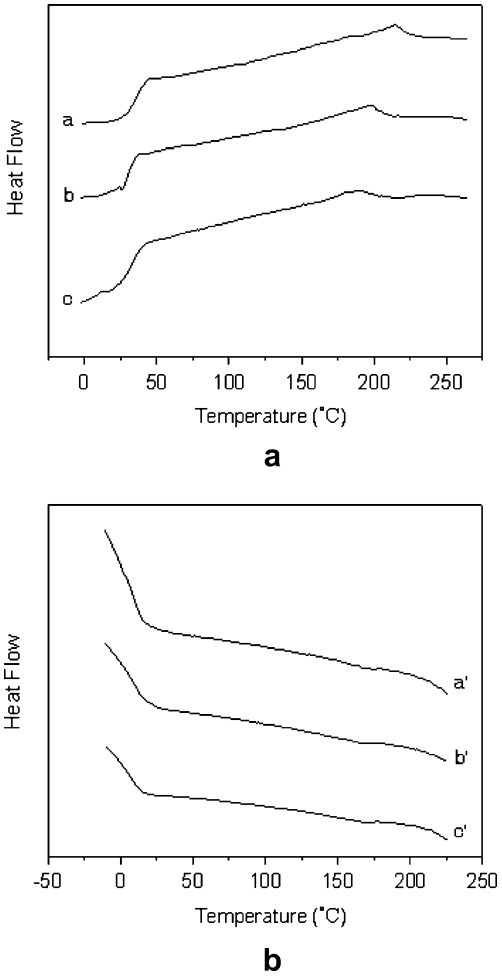

Fig. 3 DSC thermograms of representative polymers: **a** on the second heating for (*A*) **IIIP**, (*B*) **IVP**, (*C*) **VP**; **b** on the first cooling for (*A′*) **IIIP**, (*B′*) **IVP**, (*C′*) **VP**

In DSC measurements, the LC monomer **M1** showed cholesteric mesophase between 116 °C and 243 °C, as previously reported. The DSC curves of **M2** showed a melting transition at 21 °C, and no mesogenic–isotropic

Table 2 Some thermal properties and X-ray of the liquid-crystalline polymers

Sample	TGA		DSC heating and cooling[c]					$2\theta^{d}$ (°)
	Temperature[a] (°C)	Residue[b] (%)	T_g (°C)	T_i (°C)	T_{i-m} (°C)	T_{m-K} (°C)		
IP	300.1	15.2	47.3	246.3	227.6	45.6		16.54
IIP	300.8	16.9	37.4	223.4	222.8	59.8		16.59
IIIP	301.2	18.8	35.1	215.1	208.4	49.4		16.52
IVP	305.4	25.0	30.3	198.3	199.3	35.3	2.46	16.54
VP	307.6	25.9	33.4	190.4	198.7	38.7	2.45	16.49
VIP	315.4	31.0	37.4	192.4	179.9	28.9	2.45	16.53
VIIP	320.6	39.5	28.3	187.3	180.8	26.8	2.46	16.56

[a] Temperature of the samples at 5% loss weight.
[b] Residue weight of the samples on heating to 600 °C.
[c] T_g, glass-transition temperature; T_i, the isotropic temperature; T_{i-m}, phase-transition temperature from isotropic state to mesophase; T_{m-K}, mesogenic–solid phase transition temperature.
[d] X-ray diffraction (XRD) peaks of the polymers on heating to 80 °C.

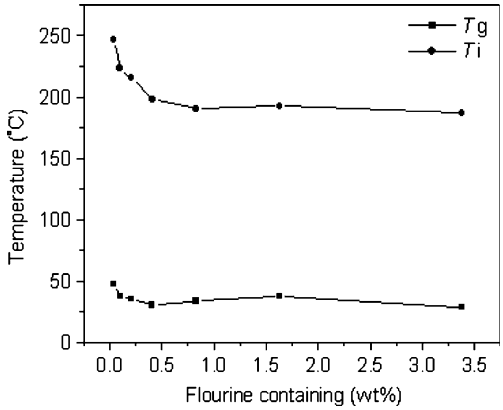

Fig. 4 Relationship between phase-transition temperatures (glass-transition and isotropic transition) and fluorine in the polymers

phase transition appeared. It indicated that **M2** is not a LC monomer.

The phase-transition temperatures of the LCPs **IP**–**VIIP**, obtained on the second heating and the first cooling scan, are summarized in Table 2. All phase transitions were reversible and did not change on repeated heating and cooling cycles. Representative DSC thermograms of the polymers on heating and cooling cycles were shown in Fig. 3. When the polymers were heated, all the polymers displayed two-phase transition temperatures corresponding to glass transition (T_g) and mesophase–isotropic phase transition (T_i) (Fig. 3a), respectively. When the polymers were cooled, they all showed two-phase transition temperatures, i.e., isotropic–mesomorphic (T_{i-m}) and mesomorphic–solid phase transitions (T_{m-K}) (Fig. 3b).

The T_g, T_i, T_{i-m}, and T_{m-K} of all polymers decreased slightly with increase of fluorinated units in the polymer systems. The relationship between phase-transition temperatures (T_g and T_i) on heating cycles and fluorine in the polymers was exhibited in Fig. 4. It suggests that the temperature range of mesophase don't change greatly for all the polymers. These kinds of side-chain liquid-crystalline polymers are composed of flexible and rigid moieties, and fluorinated groups, thus the polymer backbone, the rigidity of mesogenic units, the length of the flexible spacer, and interaction generating from fluorinated units would influence mesophase behaviors of the polymers. For the disordered systems of the atactic siloxane polymers, low temperatures induce vitrification rather than crystallization. For the polymer of this tape, the glass-transition temperature may be considered as a measure of the backbone flexibility. In our case, the polysiloxanes were graft copolymerized via hydrosilylation reaction with PMHS and one monomer containing undecylenate groups. Because the alkyl carbochains are different between **M1** and **M2**, the space groups between polysiloxane main chains and the rigid structure are different for all the polymers. Therefore, the backbone flexibility of the polymers is influenced mainly by the length of the flexible spacer. As **M2** component increased in the polymer systems, the length of the flexible spacer strengthened, resulting in a decrease of the glass-transition temperature. Besides, the strengthened flexible spacer made T_i decrease due to plasticization.

Texture analysis

The optical textures of the polymers were studied by means of POM with hot stage. The chiral polymers **IP**, **IIP**, and **IIIP** exhibited cholesteric textures when they were heated and cooled. When the sample **IP** was heated above 47 °C, eyesight became bright and LC textures appeared. The textures became obvious as the sample was heated continuously, and finally it exhibited typical oily streaks texture of the cholesteric phase (Fig. 5a). The director is basically anchored under planar conditions at the substrates, i.e., with the long molecular axis parallel to the bounding plates, which implies that the cholesteric helix axis is oriented perpendicular to the glass plates. The oily streaks texture of **IP** disappeared at 246 °C, and the sample became isotropic states. When the isotropic melt was cooled, cholesteric droplets appeared gradually (Fig. 5b). The

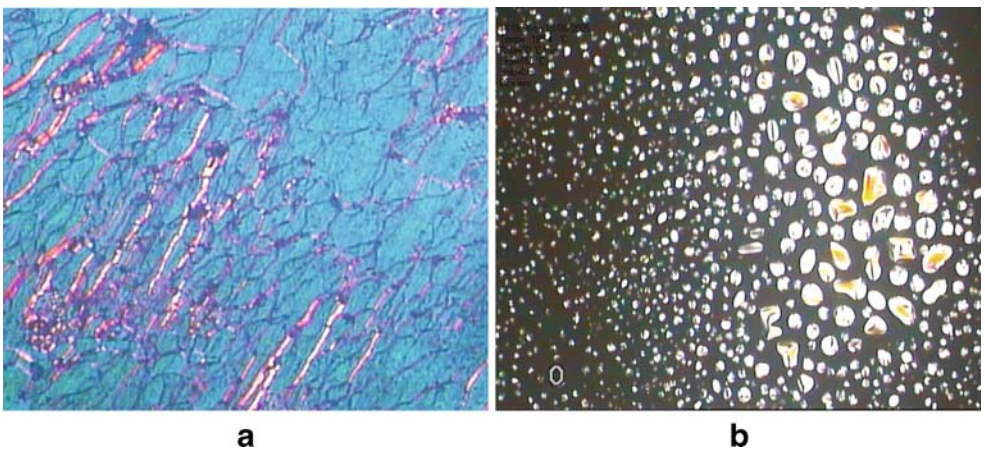

Fig. 5 Optical texture of the liquid-crystalline polymer **IP** (200×): **a** oily streaks texture on heating to 218 °C; **b** cholesteric droplets on cooling to 226 °C

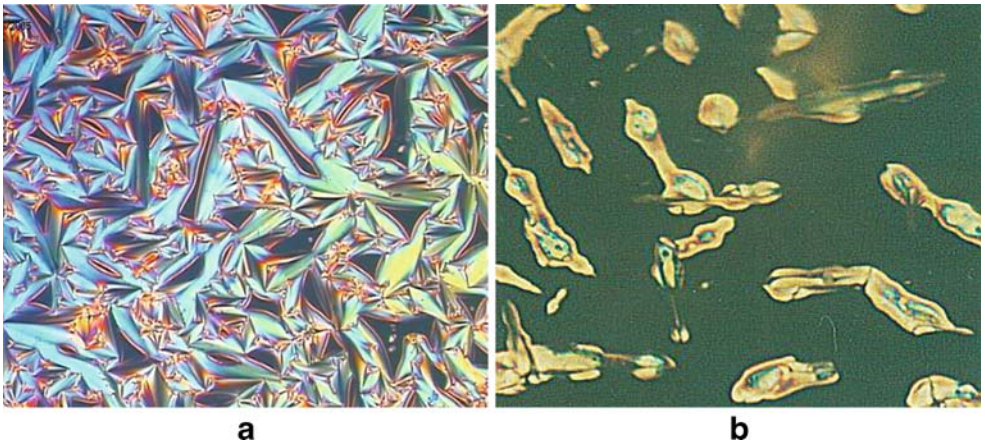

Fig. 6 Optical texture of the liquid-crystalline polymer IVP (200×): **a** fan-shaped texture on heating to 168 °C; **b** growth of SmA batonnets from the isotropic melt on cooling to 198 °C

polymers **IIP** and **IIIP** exhibited similar textures to **IP.** For the polymers **IVP**, **VP**, **VIP**, and **VIIP** that contain more fluorinate units, they showed similar smectic fan-shaped textures on heating and cooling cycles. We employed **IVP** as an example. When the sample **IVP** was heated, it showed a fan-shaped texture (Fig. 6a). The fan-shaped texture existed until the temperature of isotropic transition, and oily streaks texture didn't appear. The fan-shaped texture is the most commonly observed natural SmA appearance. Furthermore, the phase transition from the isotropic to SmA phase can easily be distinguished from that of Iso-N* [30]. While for the latter, basically, spherical nuclei were observed to grow from the black background of the isotropic melt (Fig. 5b), the direct transition to a fluid smectic phase was accomplished by the growth of batonnets (Fig. 6b).

X-ray diffraction analysis

The smectic mesophase of the polymers **IVP**, **VP**, **VIP**, and **VIIP** was also confirmed by X-ray diffraction analysis. The XRD data of all the polymers were listed in Table 2, and Fig. 7 shows representative XRD curves of samples of **IVP** and **VIIP**. XRD curves of samples of **IVP**, **VP**, **VIP**, and **VIIP** displayed sharp and strong peaks at low angle ($2\theta \approx 2.5^{o}$, d spacing 35 Å) together with a strong broad peak in wide angle ($2\theta \approx 17°$, d spacing 5.2 Å). The sharp and strong peaks at low angle indicated lamellar structure of **IVP**, **VP**, **VIP**, and **VIIP**. In general, a sharp and strong peak at low angle ($1° < 2\theta < 4°$) in small angle together with a strong broad peak in wide angle can be observed for a smectic polymer structure. For the samples **IP**, **IIP**, and **IIIP**, no sharp and strong peaks were shown at low angle, but a diffuse reflection at $2\theta \approx 4.0°$ and a broad peak appeared around $2\theta \approx 17°$ (d spacing 5.2 Å) was exhibited. The diffuse reflection located at small angles roughly corresponds to the length of the molecule whereas the wide angle reflection is related to the molecular diameter [31].

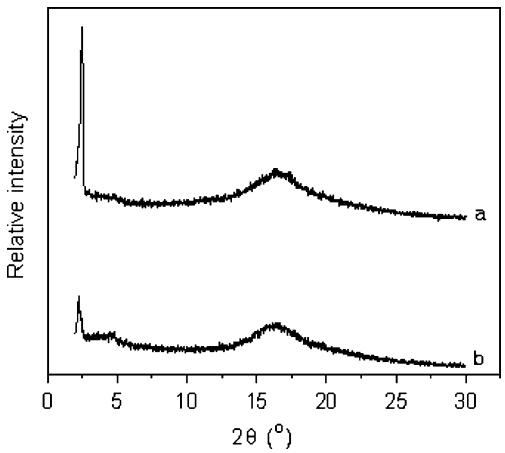

Fig. 7 Representative XRD curves of polymers on heating to 80 °C: **a VIIP**; **b IVP**

Liquid crystalline polymers are most commonly composed of flexible and rigid moieties, self-assembly and nanophase separation into specific micro-structures frequently occur due to geometric and chemical dissimilarity of the two moieties. For all the polysiloxanes, the flexible moieties include the siloxane main chains, the soft alkyl space groups and the alkyl tails. On the other hand, the mesogenic units and the fluorine-methyl-substituted phenyl benzoates constitute the rigid moieties. Because **M2** comprises of undecylenate groups and fluorine-methyl substituted phenyl benzoates, which is different to the structure of **M1**, the soft alkyl space groups and the rigid structure are different for all the polymers. For the polymers, **IP**, **IIP**, and **IIIP**, tiny **M2** were introduced into the polymer systems. Therefore, the chiral mesogens originated from **M1** would be aligned regularly in the soft polymer matrix, leading to cholesteric mesophases when the samples were heated and cooled. But the polymers, **IVP–VIIP**, with more **M2**, showed different features than **IP–IIIP**. As **M2** component increased in the polymer systems, on the one hand, the length of the flexible spacer strengthened; on the other hand, the cholesteric mesogens decreased with increase of fluorine-methyl-substituted phenyl benzoates in the polymer systems. Therefore, the

highly ordered smectic mesophases would be formed due to specific micro-structures, leading to lamellar structures. These are in agreement with the thermal behaviors, optical textures, and X-ray diffraction analysis of the polymers.

Conclusions

We synthesized a series of chiral side-chain LC polysiloxanes (**IP–VIIP**) with a cholesteric LC monomer and a non-LC monomer containing fluorinated units. The chemical structures and LC properties of the monomers and polymers were characterized by use of various experimental techniques. The chemical structures of the polymers and the content of fluorinated groups were characterized with FTIR and EA. The obtained polymers were soluble in many solvents such as toluene, xylene, THF, chloroform, and so forth. The M_n of the synthesized polymers was measured on a GPC instrument. The specific rotations of the chiral liquid-crystalline polymers were also characterized by use of optical rotation analysis. The specific rotations of all the polymers showed negative values and the specific rotation absolute values were lower than those of the chiral monomers. Thermal behaviors of the chiral fluorinated LC polysiloxanes were characterized by use of TGA and DSC. The TGA results showed that T_d was greater than 300 °C for all the polymers and the residue weight of the samples on heating to 600 °C increased slightly with increase of fluorinated units in the polymer systems. When the polymers were heated and cooled, all the polymers displayed two-phase transitions, respectively. The T_g, T_i, T_{i-m}, and T_{m-K} of all polymers decreased slightly with increase of fluorinated units in the polymer systems. The optical textures of the polymers were studied by means of POM with hot stage. The chiral polymers **IP**, **IIP**, and **IIIP** exhibited cholesteric textures when they were heated and cooled. For the polymers **IVP**, **VP**, **VIP**, and **VIIP** that contain more fluorinate units, they showed similar smectic fan-shaped textures on heating and cooling cycles. The smectic mesophase of the polymers was also characterized by X-ray diffraction analysis. XRD curves of samples of **IVP**, **VP**, **VIP**, and **VIIP** displayed sharp and strong peaks at low angle ($2\theta \approx 2.5°$, d spacing 35 Å) together with a strong broad peak in wide angle ($2\theta \approx 17°$, d spacing 5.2 Å). But no sharp and strong peaks were shown at low angle for the samples **IP**, **IIP**, and **IIIP**.

Acknowledgments The authors are grateful to National Natural Science Fundamental Committee of China and HI-Tech Research and development program (863) of China, Educational Science and Technology Program of Liaoning Province for financial support of this work.

References

1. Chung TS, Ma KX, Cheng SX (2001) Macromol Rapid Commun 22:835
2. Crevoisier GD, Fabre P, Leibler L, Tence-Girault S, Corpart JM (2002) Macromolecules 35:3880
3. Krishnan S, Kwark YJ, Ober CK (2004) Chem Rec 4:315
4. Ma KX, Chung TS (2001) J Phys Chem B 105:4145
5. Furukawa Y, Shin-ya S, Miyake H, Kishino H, Yamada M, Kato H, Sato M (2001) J Appl Polym Sci 82:3333
6. Corpart JM, Girault S, Juhue D (2001) Langmuir 17:7237
7. Gopalan P, Andruzzi L, Li X, Ober CK (2002) Macromol Chem Phys 203:1573
8. Guittard F, Givenchy ET, Geribaldi S, Cambon A (1999) J Fluorin Chem 100:85
9. Bunn CW, Howells ER (1954) Nature 174:549
10. Russell TP, Rabolt JF, Twieg RJ, Siemens RL, Farner BL (1986) Macromolecules 19:1135
11. Viney C, Twieg RJ, Russel TP, Depero LE (1989) Liq Cryst 5:1783
12. Viney C, Twieg RJ, Gordon BR, Rabolt JF (1991) Mol Cryst Liq Cryst 198:285
13. Ragnoli M, Pucci E, Bertolucci M, Gallot B, Galli G (2004) J Fluorin Chem 125:283
14. Wang J, Ober CK (1997) Macromolecules 30:7560
15. Beyou E, Babin P, Bennetau B, Dunogues J, Teyssie D, Boileau S (1994) J Polym Sci Part A: Polym Chem 32:1673
16. Volkov VV, Plate NA, Takahara A, Kajiyama T, Amaya M, Murata Y (1992) Polymer 33:1316
17. Prescher D, Thiele T, Ruhmann R, Schulz G (1995) J Fluorin Chem 74:185
18. Bracon F, Guittard F, Givenchy ET, Cambon A (1999) J Polym Sci. Part A: Polym Chem 37:4487
19. Goto H, Dai X, Narihiro H, Akagi K (2004) Macromolecules 37:2353
20. Bezborodov VS, Petrov VF (1999) Liq Cryst 26:271
21. Amabilino DB, Ramos E, Serrano J, Sierra T, Veciana J (1998) J Am Chem Soc 120:9126
22. Walba DM, Yang H, Shoemaker RK, Keller P, Shao R, Coleman DA, Jones CD, Nakata M, Clark NA (2006) Chem Mater 18:4576
23. Li CY, Cheng SZD, Ge JJ, Bai F, Zhang JZ, Mann IK, Chien LC, Harris FW, Lotz B (2000) J Am Chem Soc 122:72
24. Mruk R, Zente R (2002) Macromolecules 35:185
25. Sapich B, Stumpe J, Kricheldorf HR, Fritz A, Schonhals A (2001) Macromolecules 34:5694
26. Meng FB, Zhang BY, Xiao WQ, Hu TX (2005) J Appl Polym Sci 96:625
27. Kozlovsky M, Skarp K (2005) J Polym Sci Part B: Polym Phys 43:1779
28. Hu JS, Zhang BY, Pan W, Li YH, Ren SC (2006) J Appl Polym Sci 99:2330
29. Meng FB, Zhang BY, Liu LM, Zang BL (2003) Polymer 44:3935
30. Dierking I (2003) Textures of liquid crystals. Wiley, Weinheim, pp 91–93
31. Davidson P (1996) Prog Polym Sci 21:893